MEASUREMENT OF FRACTURE TOUGHNESS FOR FIBER COMPRESSIVE FAILURE MODE OF UD COMPOSITES UNDER HIGH RATE LOADING

P. Kuhn[1], G. Catalanotti[2], J. Xavier[2,3], R.Cidade[4], H. Koerber[1] and P.P. Camanho[5]

[1]Institute for Carbon Composites, Faculty of Mechanical Engineering, Technische Universität München, Boltzmannstraße 15, D-85748 Garching b. München, Germany
Email: kuhn@lcc.mw.tum.de, Web Page: http://www.lcc.mw.tum.de
Email: koerber@lcc.mw.tum.de
[2]INEGI, Institute of Science and Innovation in Mechanical and Industrial Engineering, Rua Dr. Roberto Frias 400, 4200-465 Porto, Portugal
Email: gcatalanotti@inegi.up.pt, Web Page: http://www.inegi.up.pt
Email: jxavier@inegi.up.pt
[3]CITAB, University of Trás-os-Montes e Alto Douro, UTAD, Quinta de Prados, 5000-801, Vila Real, Portugal
[4]PEMM/COPPE, Universidade Federal do Rio de Janeiro, Rio de Janeiro, Brasil
Email: rafaelcidade@metalmat.ufrj.br, Web Page: http://www.metalmat.ufrj.br
[5]DEMec, Faculdade de Engenharia, Universidade do Porto, Rua Dr. Roberto Frias, 4200-65 Porto, Portugal
Email: pcamanho@fe.up.pt, Web Page: http://www.fe.up.pt

Keywords: Fracture toughness, high strain rate loading, experimental techniques

Abstract

This work presents an experimental study of the compressive crack resistance curve of an unidirectional composite when submitted to dynamic loading. The data reduction couples the concepts of energy release rate, size effect law and R-curve. Double-edge notched specimens of four different sizes are used. Both split-Hopkinson pressure bar and quasi-static reference tests are performed. Under dynamic loading, the same strain rate is used for all specimen types to enable a reliable determination of the size effect. The full crack resistance curves at both investigated strain rate regimes are obtained on the basis of quasi-static fracture analysis theory. The results show that the steady state fracture toughness of the fiber compressive failure mode of the unidirectional carbon-epoxy composite material IM7-8552 is 165.6 kJ/m^2 and 101.6 kJ/m^2 under dynamic and quasi-static loading, respectively. Therefore the compressive fracture toughness is found to increase with increasing strain rate.

1. Introduction

Automotive and aeronautical composite structures are subjected to dynamic load scenarios (e.g. crash, bird strike). In order to predict the initiation and evolution of damage under dynamic loading, energy-based damage models have been recently proposed [1-5]. They have been widely accepted and are now available for static loading in commercial FE codes. These models require the specification of fracture toughness parameters for the main failure modes to predict damage evolution after the material strength has been reached.

Excerpt from ISBN 978-3-00-053387-7

For the interlaminar matrix tensile failure mode, well established static test standards [6, 7] are available and are generally used to obtain the respective fracture toughness. In addition, the experimental investigation of the dynamic interlaminar fracture toughness has received significant attention over the last decades, as summarized in [8]. However, no test standards exist to measure the static fracture toughness for compressive fiber failure and, to the knowledge of the authors, the effect of dynamic loading on this material property was not yet studied.

In this work, the methodology proposed in [9] to measure the compressive crack resistance curve is enhanced to dynamic loading. This approach uses the relations between the energy release rate, the crack resistance curve and the size-effect law.

2. Material and experimental procedures

2.1. Material and test specimens

The carbon-epoxy prepreg material HexPly IM7-8552, which is commonly used in primary aerospace components, was selected for this work. In accordance with the specified heat cycle [10], a panel with a $[90/0]_{8s}$ layup and a nominal thickness of 4 mm was cured in a hot press.

From the manufactured panel, double-edge notched compression (DENC) specimens were machined using a 1 mm diameter milling tool. A constant ratio of the geometric properties (length, width, initial crack length a_0) was held for all different specimen sizes (Figure 1).

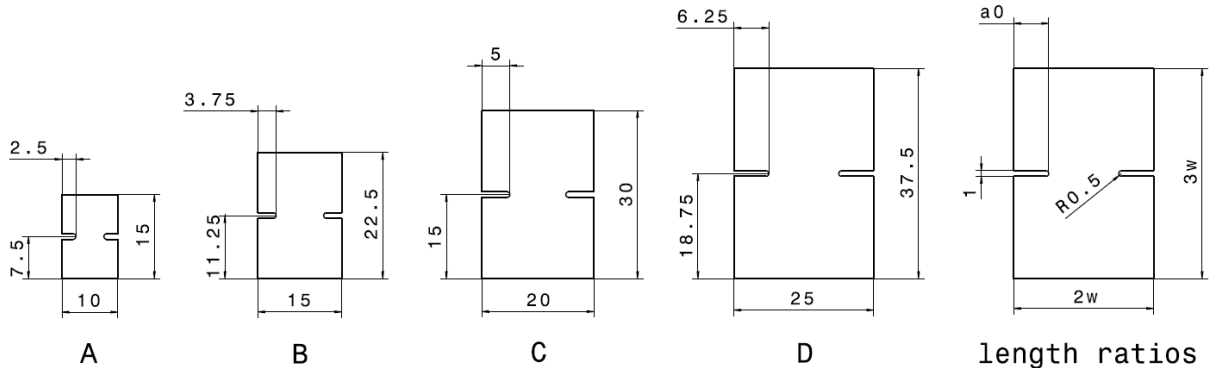

Figure 1. Dimensions of double-edge notched compression specimens

Regarding the elastic properties of the laminate under quasi-static (QS) and dynamic (HR, $\dot{\varepsilon}_s \approx 100$ 1/s) loading conditions (Table 1), and required for the subsequent data reduction, separate compression tests with unnotched specimens were performed for obtaining the Young´s modulus ($E_x = E_y$) of the balanced crossply. The shear modulus (G_{xy}) was calculated by using the classical laminate theory on basis of values from [11].

Table 1. Elastic properties of the laminate

Strain rate regime	E_x (MPa)	G_{xy} (MPa)	μ_{xy} (-)
QS	67,449	5,068	0.035
HR	67,126	6,345	0.04

Excerpt from ISBN 978-3-00-053387-7

2.1. Quasi-static experimental setup

The quasi-static (QS) reference tests were carried out on a standard electromechanical testing machine (Hegewald & Peschke Inspect Table 100), with a cross-head displacement rate of 0.15 mm/min. A self alignment system as described in [11] was used and friction between the loading parts and the specimen end-surfaces was minimized by a thin layer of molybdenum disulphide (MoS_2).

2.2. Dynamic experimental setup

The high strain rate (HR) compression tests were performed on a split-Hopkinson pressure bar (SHPB) system, as illustrated in Figure 2.The lengths of the steel striker-, incident- and transmission bars were 0.6, 2.6 and 1.3 m, respectively, and the bar diameter d_b was adapted to the tested specimen width. A Finite Element Model was used to adjusting the SHPB setup (striker velocity v_S, copper pulse shaper diameter d_{PS} and thickness t_{PS}) to ensure that the axial strain rate was the same for every specimen size, enabling a reliable determination of the strain rate effect (Table 2).

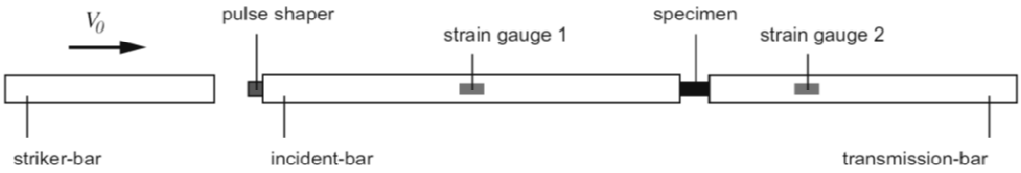

Figure 2. Split-Hopkinson pressure bar setup for dynamic tests.

Table 2. SHPB Parameter

Specimen type	w (mm)	d_b (mm)	v_S (m/s)	Pulse Shaper dimensions (mm)	
				d_{PS}	t_{PS}
A	5	16	8.6	6	1.5
B	7.5	18	9.4	8	1.5
C	10	18	11.0	10	2.0
D	12.5	25	12.2	10	2.0

2.3. Data reduction methods

For the quasi-static tests the ultimate remote stress σ_u was calculated by dividing the peak load P_u measured from the load cell of the testing machine by the specimen cross-section in the unnotched regions A_s. For the high rate tests the axial stress components σ_s at the specimen/transmission-bar and incident-bar/specimen interfaces can be calculated by using 1-wave and 2-wave-analysis,respectively, as [12]

$$\sigma_{s1} = \frac{A_b}{A_s} E_b \varepsilon_T, \tag{1}$$

$$\sigma_{s2} = \frac{A_b}{A_s} E_b (\varepsilon_I + \varepsilon_R). \tag{2}$$

where A_b is the bar cross-section; E_b is the elastic wave Young's modulus of the bar material; ε_I, ε_R and ε_T are the incident, reflected and transmitted bar-strain waves, respectively. As both terms (Eq. 1, Eq. 2) were used for the check and confirmation of specimen stress-equilibrium, ultimate stress was

Excerpt from ISBN 978-3-00-053387-7

calculated just from Eq. 2 due to the smooth transmitted wave signal. The axial strain rate $\dot{\varepsilon}_s$ along the unnotched part of the specimen was calculated as given in [12]

$$\dot{\varepsilon}_s = \frac{c_b}{l_s}(-\varepsilon_I + \varepsilon_R + \varepsilon_T) \tag{3}$$

where c_b denotes the elastic wave velocity of the bars and l_s is the specimen length.

3. Experimental results

For each specimen type and strain rate regime, three valid tests were performed. As expected, all specimens failed due to compressive fracture along the direction of the initial notch and a pronounced strain rate effect on the measured ultimate remote stress occured for all tested specimen sizes (Table 3).

Table 3. Summary of ultimate remote stress measured for quasi-static and dynamic loading

Specimen label		A	B	C	D
QS	σ_u (MPa)	310	264	253	234
	STDV (σ_u) (MPa)	27	16	3	14
HR	σ_u (MPa)	380	357	325	299
	STDV (σ_u) (MPa)	23	9	5	7

Figure 4a shows the axial stress curves over time for a specimen of type C during high rate loading, calculated with Eq. 1 and Eq. 2. The correlation of the two signals indicates that, after an initial ringing-up, the DENC-specimens are in stress-equilibrium before damage initiation. In addition, approximately the same strain rate ($\dot{\varepsilon}_s \approx 100$ 1/s) was achieved for all specimen types, before the occurance of failure (Figure 4b).

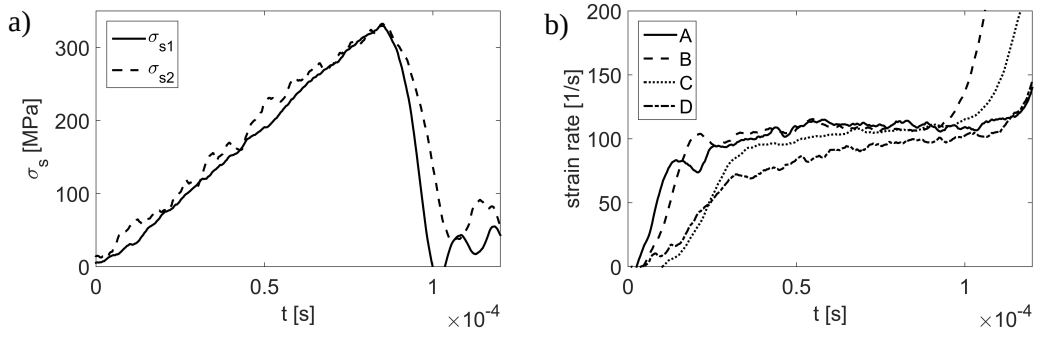

Figure 4. Calculated specimen stress on basis of 1-wave and 2-wave analysis (a) and typical strain rate - time curves for all specimen types (b)

4. Obtaining the R-curve

Following the approach described in [9], the R-curve can be calculated on the basis of the obtained ultimate stress of the different specimen sizes, using the relation between the energy release rate, the size effect law and the R-curve [13]. According to [14], quasi-static fracture mechanics theory is applicable for dynamic fracture toughness measurement under the condition of stress-equilibrium and was therefore used in this work.

Excerpt from ISBN 978-3-00-053387-7

Based on [15], the energy release rate in a two-dimensional balanced crossply under tensile or compressive loading normal to the fracture surface (mode I) can be written as

$$G_I|\sigma_u(a+\Delta a) = \frac{1}{E}\sqrt{\frac{1+\rho}{2}}w\sigma_u(w)^2\phi\left(\alpha_0+\frac{\Delta a}{w},\rho\right) \tag{4}$$

where E denotes the laminate Young´s modulus ($E = E_x = E_y$), w is the characteristic specimen size (Figure 1), $\alpha_0 = a_0/w$, Δa is the propagating crack length and ρ is the dimensionless elastic parameter defined as [15]

$$\rho = \frac{2s_{12}+s_{66}}{2\sqrt{s_{11}s_{22}}}. \tag{5}$$

In Eq. 4, ϕ is the correction factor of orthotropy and geometry of the material and can be calculated by applying the Virtual Crack Closure Technique (VCCT) [16] in a simplified Finite Element Model of the DENC specimen [9]. The relation between the ultimate remote stress and the characteristic specimen size $\sigma_u(w)$ is defined by the size effect law. According to [9], the size effect law of IM7-8552 under compressive loading can be expressed as

$$\sigma_u = (mw+q)^{-\frac{1}{2}} \tag{6}$$

where m and q are the slope and the intercept of the linear fit, respectively. Figure 5a shows the linear fit of the test data of the two investigated strain rate regimes and the corresponding line coefficients in Eq. 6 are listed in Table 4. Knowing all the input parameters of Eq. 4, the energy release rate curves for different w can be drawn. Finally, the R-curve of the laminate is the envelope of the family of curves of the energy release rate. According to [17], the R-curve of the 0° plies (R_0) is simply twice of R laminate (for the laminate chosen in this study). The quasi-static and dynamic R-curves for the fiber-compressive failure of a UD IM7-8552 ply are plotted in Figure 5b.

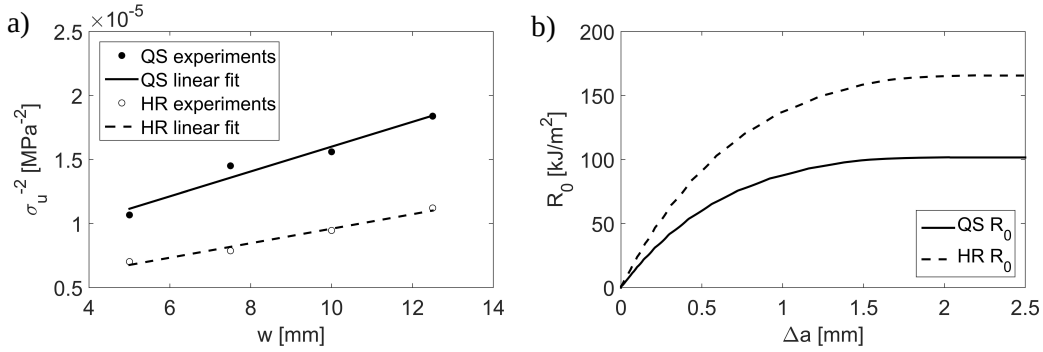

Figure 5. σ_u^{-2} vs. w and linear curve fitting (a) and R-curves of the 0°-plies (b)

The steady state value of the fracture toughness R_{ss} can be obtained as [9]:

$$R_{ss} = \lim_{n\to\infty} R_0 = \frac{\sqrt{2(1+\rho)}}{E}\frac{\phi_0}{m} \tag{7}$$

where $\phi_0 = \phi|_{\alpha=\alpha 0}$. The values of R_{ss} at both strain rate regimes are listed in Table 4.

Excerpt from ISBN 978-3-00-053387-7

Table 4. Line coefficients of the size effect law and R_{ss}

Strain rate regime	Line coefficients		R_{ss}
	m	*q*	
QS	9.70e-7	6.31e-6	101.6
HR	5.67e-7	3.93e-6	165.6

5. Conclusion

The fracture toughness of the fiber compressive failure mode of the carbon-epoxy material IM7-8552 under high rate loading was determined in this work. For this purpose, the methodology proposed in [9] was enhanced to dynamic loading. The required dynamic test data was obtained from split-Hopkinson pressure bar tests using double-edge notched specimens with four different sizes. At the high strain rate a steady state fracture toughness value of 165.6 kJ/m^2 was found, which is significantly higher than the fracture toughness for quasi-static loading (101.6 kJ/m^2).

The methodology and results of the presented work can be used to further enhance state-of-the-art composite material models and can contribute to a further understanding of the complex material response of composite materials.

References

[1] I. Lapczyk and J. Hurtado. Progressive damage modeling in fiber-reinforced materials. *Composites: Part A*, 38:2333-2341, 2007.
[2] M. Vogler, R. Rolfes and P.P. Camanho. Modeling the inelastic deformation and fracture of polymer composites part I: Plasticity model. *Mech Mater*, 59:50–64, 2013.
[3] P.P. Camanho, M.A. Bessa, G. Catalanotti, M. Vogler and R. Rolfes. Modeling the inelastic deformation and fracture of polymer composites part II: Smeared crack model. *Mech Mater*, 59:36–49, 2013.
[4] S.T. Pinho, L. Iannucci and P. Robinson. Physically-based failure models and criteria for laminated fibre-reinforced composites with emphasis on fibre kinking: Part I: Development. *Composites Part A*, 37:63-73, 2006.
[5] P. Maimi, P.P. Camanho, J.A. Mayugo and C.G. Davila, A continuum damage model for composite laminates: Part I – Constitutive model, *Mechanics of Materials*, 39:897-908, 2007.
[6] ASTM D5528. Standard test method for mode I interlaminar fracture toughness of unidirectional fiber-reinforced polymer matrix composites. West Conshohocken PA, USA: ASTM, 2013.
[7] DIN EN 6033- Aerospace series - Carbon fibre reinforced plastics - Test method - Determination of interlaminar fracture toughness energy - Mode I G[Ic]. German and English version FprEN 6033:2013, Deutsches Institut für Normung e.V., 2013.
[8] G.C. Jacob, J.M. Starbuck, J.F. Fellers, S. Simunovic and R.G. Boeman. The Effect of Loading Rate on the Fracture Toughness of Fiber Reinforced Polymer Composites. *Journal of Applied Polymer Science*, 96:899-904, 2005.
[9] G. Catalanotti, J. Xavier and P.P. Camanho. Measurement of the compressive crack resistance curve of composites using the size effect law. *Composites: Part A*, 56:300-307, 2014.
[10] Material Data Sheet. HexPly 8852 Product Data, 2013.
[11] H. Koerber, J. Xavier and P.P. Camanho. High strain rate characterisation of unidirectional carbon-epoxy IM7-8552 in transverse compression and in-plane shear using digital image correlation. *Mechanics of Materials*, 42:1004-1019, 2010.
[12] G.T. Gray III. Classic split-Hopkinson pressure bar testing. In: *ASM Handbook, Mechanical Testing and Evaluation.* ASM Int.,Materials Park OH, 462–476, 2000.

Excerpt from ISBN 978-3-00-053387-7

[13] Z.P. Bažant and J. Planas. *Fracture and Size Effect in Concrete and Other Quasibrittle Materials.* CRC Press, 1997.

[14] F. Jiang and K.S. Vecchio. Hopkinson Bar Loaded Fracture Experimental Technique: A Critical Review of Dynamic Fracture Toughness Tests. *Applied Mechanics Reviews*, 62:1-39, 2009.

[15] Z. Suo, G. Bao, B. Fan and T.C. Wang. Orthotropy rescaling and implications for fracture in composites. *Int. J. Solids Structures*, 28:235-248, 1990.

[16] R. Krueger. The virtual crack closure technique: History, approach and applications. *Technical Report NASA/CR-2002-211628 ICASE Report No. 2002-10*, 2002

[17] S.T. Pinho, P. Robinson and L. Iannucci. Fracture toughness of the tensile and compressive fiber failure modes in laminated composites. *Composites Science and Technology*, 66:2069-2079, 2006

Excerpt from ISBN 978-3-00-053387-7